

**Mixing generated by Faraday instability between miscible liquids**Sakir Amiroudine<sup>\*</sup>*University of Bordeaux, Institut de Mécanique et d'Ingénierie-TREFLE, UMR CNRS 5295  
16 Avenue Pey-Berland, Pessac Cedex, F-33607, France*Farzam Zoueshtiagh<sup>†</sup>*University of Lille 1, Institut d'Electronique, de Microélectronique et de Nanotechnologie (IEMN) UMR CNRS 8520  
Avenue Poincaré, F-59652 Villeneuve d'Ascq, France*Ranga Narayanan<sup>‡</sup>*University of Florida, Gainesville, Florida 32611, USA*

(Received 7 July 2011; revised manuscript received 12 December 2011; published 27 January 2012)

The mixing between two miscible liquids subject to vertical vibrations is studied by way of experiments and a two-dimensional numerical model. The experimental setup consisted of a rectangular cell in which the lighter fluid was placed above the denser one. The diffuse interface was then visualized by a high-speed camera. After an initial period of diffusion growth, the interface becomes unstable with a defined wavelength, which depends on the amplitude and frequency of the acceleration. The waviness of the interfacial region disappears once the mixing of the two fluids takes place. The mixing is characterized by a mixing layer thickness (MLT) which measures the thickness of the mixed region between the two pure fluid domains. We find that the MLT shows an exponential growth with time due to an initial fingering that appears at the interface and then a growth with a defined slope after the mixing takes place. The MLT also increases with amplitude of driving motion. Experimentally determined MLTs are always greater than those determined by computations since the latter assume a jump discontinuity between the fluids prior to shaking, whereas in an experiment an initial diffusive region establishes itself prior to shaking and this is destabilizing. In addition, it is found from computations that mixing is best for low gravity levels at earlier times and high gravity levels at longer times. Explanations are advanced for each of these observations.

DOI: [10.1103/PhysRevE.85.016326](https://doi.org/10.1103/PhysRevE.85.016326)

PACS number(s): 47.51.+a, 68.05.-n, 33.57.+c, 78.20.Ls

**I. INTRODUCTION**

The generation of waves near the diffuse interface of two immiscible liquid layers that are subjected to vertical vibrations is known as the Faraday instability [1,2]. This instability occurs on account of a resonance that is set up when there is a tuning of the imposed frequency with the natural frequency of the free surface, which possesses surface potential energy. This type of instability can also occur between two miscible liquids with different densities [3]. In the experiments of Zoueshtiagh *et al.* [3], where miscible fluid systems were studied, the amplitude of the instability grew, which then led to the mixing of the liquids. The waviness of the interface finally disappeared once the two liquids were fully mixed over a volume, considerably larger than the initial diffuse region. In this paper, we report an experimental and numerical study of Faraday instability used as a mixing tool when the applied acceleration is perpendicular to the interface. In particular, we investigate the mixing efficiency of the instability by measuring the size of the volume where the two liquids were fully mixed as a function of time, under different external vibration parameters. A study of the mixing layer thickness (MLT) based on experiments and numerical computations is presented. The numerical study is extended to the case

where gravity is a varying parameter, with potential space applications.

**II. EXPERIMENTAL SET-UP**

The test cell depicted in Fig. 1(a) consists of a Plexiglas cell of  $8 \times 4 \times 2 \text{ cm}^3$ , which was filled until level 1 with the heavier of the two fluids. From level 1 to the top, the cell was filled through the side hole 2 with the lighter of the two fluids. Air bubbles inside the cell were evacuated via the vent or “gas exiting hole” at the top of the cell. Because of the density gradient between the two liquids at their interface, the latter was easily observable with ordinary lighting. The cell was typically shaken 5 min after the start of injection of the lighter fluid into the cell with the initial thickness of the diffuse interface of the order of millimeters. This time corresponded to the time necessary to slowly fill the cell without drastically perturbing the interface. The range of amplitudes,  $A$ , and frequencies,  $f$ , of the oscillations were  $A \leq 12 \text{ cm}$  and  $f \leq 10 \text{ Hz}$  (for more details on the experimental setup, cf. Ref. [3]). The motion of the interface was observed by a high-speed camera at 150, 200, or 250 images per second with an exposure time of  $250 \mu\text{s}$  [see Fig. 1(b)]. The recorded images were digitized and calibrated into length scales from which the size of the instability (wavelengths) and mixing zone thickness were measured. To estimate the behavior of mixing zone thickness with imposed amplitude and frequency, a mathematical model is proposed. A 2D model meets the

<sup>\*</sup>sakir.amiroudine@u-bordeaux1.fr<sup>†</sup>farzam.zoueshtiagh@univ-lille1.fr<sup>‡</sup>ranga@ufl.edu

purposes of our study on qualitative grounds and it is to this that we now turn.

### III. MATHEMATICAL MODEL

We consider a 2D rectangular cavity [see Fig. 1(c)] to model the experimental cell of Fig. 1(a). This cavity is filled with the two miscible liquids (here brine and pure water). The entire container is subjected to vibration of amplitude  $A$  and frequency  $\omega = 2\pi f$ . The scaled equations are written below.

$$\left. \begin{aligned} \frac{\partial \rho}{\partial t} + \nabla \cdot (\rho \vec{V}) &= 0 \\ \rho \left[ \frac{\partial \vec{V}}{\partial t} + (\vec{V} \cdot \nabla) \vec{V} \right] &= -\nabla P + \frac{\Delta \vec{V}}{\text{Re}} - \rho \left[ \frac{1}{\text{Fr}^2} - \frac{\sin(W_0 t)}{\text{Fr}_v^2} \right] \vec{j} \\ \rho \left[ \frac{\partial \varpi_I}{\partial t} + \vec{V} \cdot \nabla \varpi_I \right] &= \frac{1}{\text{ReSc}} \nabla \cdot (\rho \nabla \varpi_I) \end{aligned} \right\} \quad (1)$$

In the above equations, all the variables are dimensionless:  $\vec{V}$  is the velocity vector whose horizontal and vertical components are denoted by  $U$  and  $V$ , respectively,  $t$  is the time,  $P$  is the pressure field, and  $\rho = 1 + \gamma(\varpi_I - 1)$  is the mixture density. Here,  $\varpi_I$  is the mass fraction of the heavier species and  $\gamma$  is given by  $\gamma = (\rho_I - \rho_{II})/\rho_I$ , where  $\rho_I$  is the density of the heavy species. To render the modeling equations in scaled form, we define length, time, and velocity scales. The length scale “ $L$ ” is given by  $\sqrt{D t_0}$ , the time scale by  $t_{\text{ref}} = L^2/\nu$  and the velocity scale by  $U_{\text{ref}} = \nu/L$ , where  $D$  and  $\nu$  are the mass diffusivity and kinematic viscosity, respectively. Here,  $t_0$  is the experimental wait time before the oscillations are imposed, which basically corresponds to the time of mass diffusion. The different dimensionless groups appearing in the above equations are the following:  $\text{Fr} = U_{\text{ref}}/\sqrt{Lg}$  (Froude number), where  $g$  is the gravitational acceleration,  $\text{Sc} = \nu/D$  (Schmidt

number),  $W_0 = 2\pi f t_{\text{ref}}$  (Womersley number),  $\text{Re} = L U_{\text{ref}}/\nu$  (Reynolds number), and  $\text{Fr}_v = U_{\text{ref}}/\sqrt{LA(2\pi f)^2}$  (vibration Froude number). We see that the scale factors make the Reynolds number,  $\text{Re}$ , equal to unity. The above system of equations is solved with the following dimensionless boundary conditions:

$$\left. \begin{aligned} y=0, \quad U=0, V=0, \varpi_I=1 \\ y=H/L, \quad U=0, V=0, \varpi_I=0 \\ x=0, W/L, \quad U=0, V=0, \frac{\partial \varpi_I}{\partial x}=0 \end{aligned} \right\} \quad (2)$$

The mixing layer thickness (MLT) is calculated by considering the average density in the  $x$  direction as

$$\bar{\rho}(y,t) = \frac{1}{W/L} \int_0^{W/L} \rho(x,y,t) dx. \quad (3)$$

The MLT is then defined by

$$d(t) = y_{\text{max}}(t) - y_{\text{min}}(t), \quad (4)$$

where  $y_{\text{min}}(t)$  is calculated by the condition  $[1 - \bar{\rho}(y,t)] > \epsilon$  and  $y_{\text{max}}(t)$  by  $\bar{\rho}(y,t) < \epsilon$ . The value of  $\epsilon$  is taken here as  $10^{-5}$ . In other words,  $y_{\text{min}}$  is the location below which the heavier fluid is very nearly uniform; likewise,  $y_{\text{max}}$  is the location above which the lighter fluid is nearly uniform, the acceptable deviation from uniformity being given by  $\epsilon$ .

Equations (1) and (2) are solved by a finite volume method using the SIMPLER algorithm [4] in a staggered mesh. The space discretization uses the power-law scheme [5] and time discretization is of the first-order Euler type. The effect of the grid size was carefully tested for convergence. A nonuniform mesh is used in order to capture the phenomena at the interface and near the walls. The vibrational boundary layer thickness is of the order of  $\delta_{\text{vib}} = \sqrt{\nu/(\pi f)} \approx 178 \mu\text{m}$  for a maximum frequency of  $f = 10$  Hz and kinematic viscosity of 1 cSt. Therefore, for all cases the nonuniform mesh has  $80 \times 80$  points and the first point of the mesh is at around  $150 \mu\text{m}$ . The time step chosen is equal to  $10^{-3}$  s, which is very small with respect to all of the characteristic time scales.

### IV. RESULTS

The study undertaken in a previous paper [3] has shown that when a miscible two-fluid system is subject to vertical vibrations, the interface showed waviness whose wavelength decreased as the acceleration increased. The amplitude of the fingers grew in time and then the mixing of the fluids took place. In this paper, we characterize the mixing by the evolution of MLT as a function of time, acceleration, and level of the gravity.

In order to determine experimentally a temporal evolution of MLT in two dimensions, thus accounting for the waviness of the interface, the MLT was evaluated in some experiments and the data are compared to the numerical results. The method consisted of measuring the minimum and the maximum  $y$  coordinate in each image, where the bottom and top limits of the liquid mixing zone could be observed. This method is equivalent to the calculation of MLT in numerical simulations using Eq. (4). The results are presented in Fig. 2, where the evolution of the MLT is plotted as a function of time for the case of  $A = 1$  cm and  $f = 5$  Hz. The graph shows

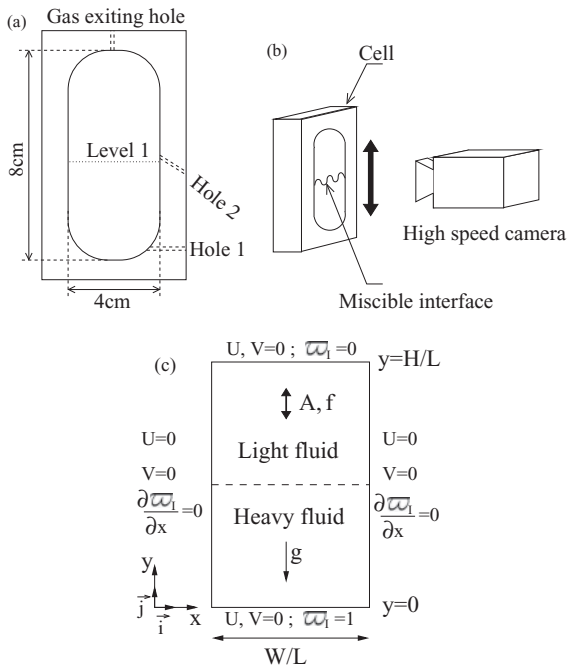


FIG. 1. Sketch of (a) the test cell and (b) the experimental setup. (c) The geometry and the boundary conditions of the numerical problem.

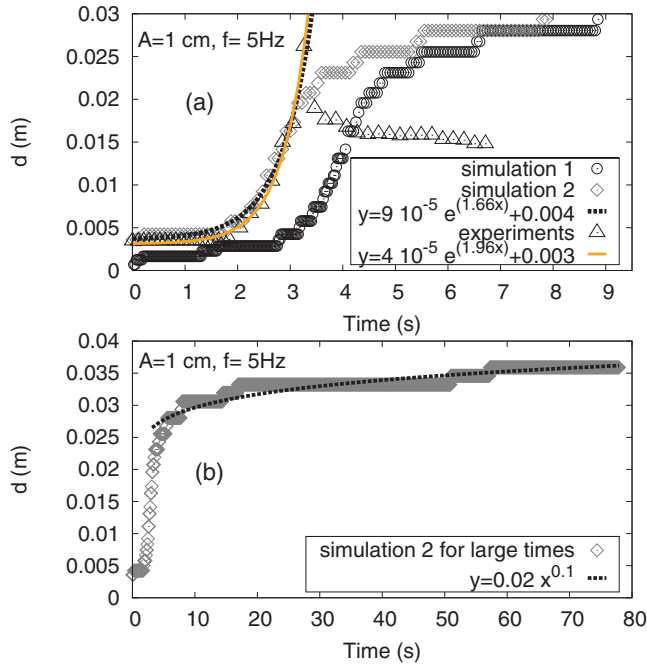


FIG. 2. (Color online) Experimental and numerical MLT,  $d$ , as a function of time for an amplitude of  $A = 1$  cm and frequency of  $f = 5$  Hz. (a) Comparison between experiments and simulations 1 and 2 corresponding to sharp and diffuse initial interfaces, respectively. (b) Numerical MLT for larger simulation times.

that there are two distinct regimes characterizing the MLT. The first regime corresponds to an exponential state where fingers of the instability are at the origin of any mixing in the system. This exponential behavior is similar to that found by Siddavaram and Homsy [6] in which the setup was different as the acceleration was parallel to the interface. The second regime starts after the fingers have vanished, i.e., after the instability has vanished. The growth of MLT in this regime can only be observed when the mixing by the instability (regime 1) has not invaded the whole cell. This is the case for Fig. 2. The numerical data obtained for large simulation times show a saturation of MLT in regime 2 [see Fig. 2(b)]. In this second regime, the experimental data [Fig. 2(a)] appear to generally underestimate the MLT and seem to even decrease with time. This is due to increasing uncertainty in image readings when the mixing takes place. Indeed, as the experimental visualization of the MLT relies on the gradient of density at the interface [3], the density gradient decreases as the mixing takes place and it becomes technically more difficult to evaluate the MLT.

The graph in Fig. 2 shows that the instability arises at shorter times in the experiments than in the simulations with a sharp initial interface (simulation 1). This is understandable since in the experiments, unlike in the simulations with a sharp interface [simulation 1 in Fig. 2(a)], there is a nonzero initial interface layer thickness [3]. The origin of the instability can be traced to the existence of a diffusion layer prior to shaking and in this sense the instability is akin to the Bénard problem. In simulation 2, this initial diffusion length is taken into account by considering a simulation for a given time period without activating the acceleration. As soon as the

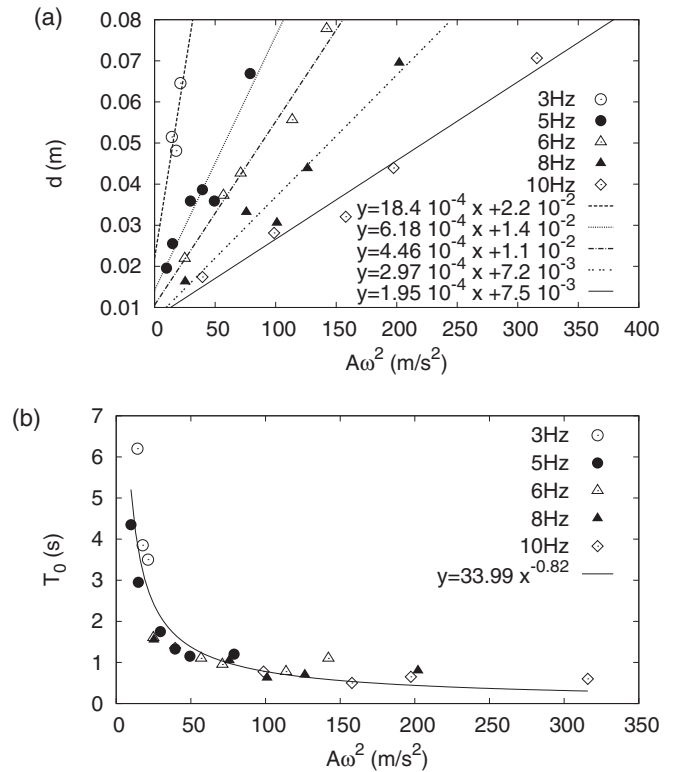


FIG. 3. (a) Numerical MLT,  $d$ , at the end of the exponential growth as a function of the acceleration. (b) Time at the end of the exponential growth as a function of acceleration in the numerical simulation.

initial diffusion length in the simulations reaches that of the experiments, the acceleration is then set on. Given the difficulty in estimating accurately the MLT in the experiments, this result is remarkable and expresses good agreement between experiments and simulations for the regime 1 where instability controls the mixing mechanism.

Figure 3(a) shows the MLT obtained at the end of the exponential growth as a function of the acceleration level for different fixed frequencies. The increase in MLT with acceleration implies that the MLT increases with the amplitude, a control variable that occurs only linearly in the modeling equations. The rise in the curve follows from an increase in the instability with acceleration. After the instability commences, the mixing takes place and the concentration gradients are reduced. Now these concentration gradients are the very cause of the instability and so the reduction of the gradients causes a termination of the instability. In other words, the instability sows the seeds of its own destruction. By this argument, one must expect the duration of the instability to decrease with acceleration, no matter how this acceleration is achieved. This, too, is seen clearly in Fig. 3(b), which shows the time,  $T_0$ , required for each system to reach the end of the exponential growth behavior. This time shows a power-law type decrease as the acceleration of the vibrations is increased. In addition to the linear behavior of MLT with  $A\omega^2$ , it appears that for the same accelerations, larger values of MLT are obtained with smaller  $\omega$ . Indeed, for high-frequency runs, the fingers developed at the interface do not have enough time to “travel far” in the cell before the direction of the acceleration

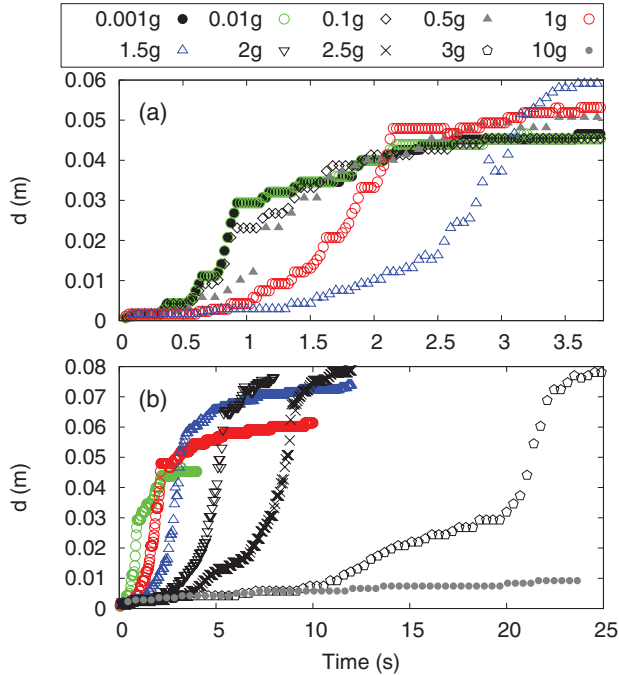


FIG. 4. (Color online) Numerical MLT,  $d$ , as a function of time for different level of gravity for a fixed acceleration of ( $\Gamma = 25.26 \text{ ms}^{-2}$ ). The upper and lower graphs show MLT behavior for small and large times, respectively. For the sake of clarity, some of the data were not included in both graphs. Simulation parameters are  $A = 4 \text{ cm}$  and  $f = 4 \text{ Hz}$ .

and, thus, the direction of finger movement is reversed. Therefore, the extent of MLTs reached in the cell for high frequency runs remain smaller than those of low-frequency experiments.

Figure 4 shows the calculated MLT as a function of time for different levels of gravity (from 0.001 to 10 g) and for a fixed acceleration ( $\Gamma = 25.26 \text{ m.s}^{-2}$ ). It appears that with increasing the level of gravity, the development of the instability is delayed as the gravity has a stabilization effect. However, once the instability emerges, its “lifetime,” which corresponds to the exponential growth state, increases. This suggests that the mixing at the interface is retarded for larger gravity level. This in turn helps to keep a sufficiently large gradient of density at the interface and, therefore, the instability can endure for longer time. As a consequence, the MLT that is obtained at the end of the exponential growth is larger for larger gravity level [Fig. 4(b)].

It is interesting to note that at earlier times [less than about 1.5 s; see Fig. 4(a)], the MLT has higher values for low-gravity levels than for high-gravity levels. As time progresses, this situation reverses as the mixing is higher for higher values of the gravity. The waviness appears indeed at the earlier times for lower values of the gravity (say 0.01 g) than for higher values of the gravity (say 1 g) due to the stabilizing buoyancy force in the case of the latter. For the case of higher values of gravity, the thickness of the diffusion layer grows as time progresses and when the instability starts, the mixing invades most of the cell more rapidly because a thicker diffuse layer obtains and this renders the fingering process unstable (cf., the discussion of Fig. 2). Thus, at a fixed value of acceleration ( $\Gamma \approx 2.57 \text{ g}$ ),

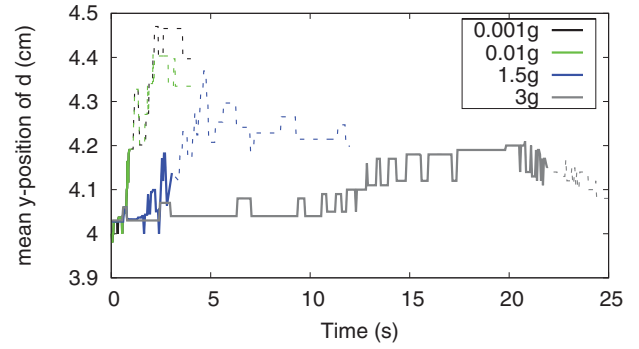


FIG. 5. (Color online) Numerical mean vertical position of  $d$  as a function of time for different level of gravity for a fixed acceleration of ( $\Gamma = 25.26 \text{ ms}^{-2}$ ). The solid and dashed lines, respectively, highlight the exponential (regime 1) and the slow-growth (regime 2) regimes in the simulations. Simulation parameters are  $A = 4 \text{ cm}$  and  $f = 4 \text{ Hz}$ .

the mixing is better for large values of the gravity level if one waits for longer times.

Figure 5 shows the mean vertical position of MLT as a function of time. In this figure, the solid and dashed lines highlight the exponential (regime 1) and the slow-growth (regime 2) regimes in the simulations. It appears that the mean vertical position of MLT at the end of the exponential state is nearly identical for any level of gravity despite the fact that the absolute value of MLT increases with increasing gravity level (Fig. 5). This suggests that the motion of mean MLT position depends on excitation parameters rather than the level of gravity.

In the regime 2 the position of MLT is seen to move toward the top of the cell for all levels of gravity (see Fig. 5), but this movement is less important for large values of gravity.

## V. CONCLUSION

Experimental runs and numerical simulations on the interfacial instability between two miscible liquids that are subject to accelerations have been performed. It has been shown in a previous paper [3] that the wavelength of the interface decreases when the magnitude of the acceleration increases, much like the case of two immiscible fluids [2]. The amplitude of the waves at the interface grows in both directions as time goes on and then the fingers mix. A study of this mixing process has been undertaken here as a function of time, levels of acceleration, and gravity. Several key observations were obtained from this study. First, the mixing layer thickness grows exponentially with time as the fingering takes place at the interface. This is followed by a smaller rate of growth where the motion from the instability quenches. Second, the MLT increases with the amplitude of the external motion. Further, for a fixed amplitude the MLT increases with a decrease in frequency. Third, numerical simulations that assume a jump discontinuity between the fluids at the beginning show more stability compared to the experiments wherein the starting profile has a diffusion region between the fluids. This follows from the fact that a gradient or diffusion profile prior to external forcing enhances instability much like the Bénard problem.

Last, numerical computations show that large gravity leads to stability at earlier times wherein diffusion gradients can more easily establish; in turn, these very diffusional gradients enhance destabilization at long times with the result that the MLT for large gravity is greater at long times.

#### ACKNOWLEDGMENTS

Support from NSF-OISE 0968313, Partner University Fund, CNRS-CNES, and Marie Curie International Research Staff Exchange Scheme Fellowship within the 7th European Community Framework Programme are acknowledged.

- 
- [1] T. B. Benjamin and F. Ursell, *Proc. R. Soc. London, Ser. A* **225**, 505 (1954).  
[2] K. Kumar and L. S. Tuckerman, *J. Fluid Mech.* **329**, 49 (1994).  
[3] F. Zoueshtiagh, S. Amiroudine, and R. Narayanan, *J. Fluid Mech.* **628**, 43 (2009).  
[4] S. Amiroudine, J. Ouazzani, B. Zappoli, and P. Carlès, *Eur. J. Mech. B/Fluids* **16**, 665 (1997).  
[5] S. Patankar, *Numerical Heat Transfer and Fluid Flows* (MacGraw Hill, 1980).  
[6] V. K. Siddavaram and G. M. Homsy, *J. Fluid Mech.* **562**, 445 (2006).